ELSEVIER

Journal of Hazardous Materials B135 (2006) 210–217

Journal of Hazardous Materials

www.elsevier.com/locate/jhazmat

Adsorption of MTBE from contaminated water by carbonaceous resins and mordenite zeolite

Hsu-Wen Hung *, Tsair-Fuh Lin

Department of Environmental Engineering, National Cheng Kung University, Tainan City 70101, Taiwan, ROC

Received 22 April 2005; received in revised form 12 November 2005; accepted 18 November 2005
Available online 18 January 2006

Abstract

Equilibrium and kinetic adsorption of methyl *tert*-butyl ether (MTBE) onto two carbonaceous resins and one zeolite was elucidated in this study. The Freundlich isotherm is adequate for describing the adsorption equilibrium of MTBE onto all the tested adsorbents in deionized water and natural waters. The resins of Ambersorb 563 and 572 have the highest adsorption capacity and almost twice the capacity of mordenite in deionized water. A different extent of NOM competition with MTBE was found for the carbonaceous resins in natural waters. For mordenite, no competitive adsorption was observed in natural water. The ideal adsorbed solution theory combined with equivalent background compound (IAST-EBC) model successfully described and predicted the adsorption of MTBE onto the carbonaceous resins in natural waters. The pore diffusion and micropore diffusion model fit the experimental data fairly well and successfully predicted the transport of MTBE within the adsorbent under different operating conditions. The small tortuosity factor between 1.2 and 2.3 of the resins for the diffusion of MTBE was observed, indicating a superior transport property for the carbonaceous resins in natural waters. The intracrystalline diffusivity of MTBE in natural water was much slower than that in deionized water, only 1/10 in STL and 1/3 in FS natural water, since the aperture entrances of mordenite was appreciably hindered by NOM.

Keywords: Adsorption; MTBE; NOM; Resin; Zeolite

1. Introduction

Methyl *tert*-butyl ether (MTBE) is the most common oxygenated fuel additive used to increase the octane rating and to enhance the combustion efficiency of gasoline. Due to its high water solubility, slow biodegradability, low Henry's law constant, and small partition coefficient, MTBE is relatively stable and recalcitrant compared to many other gasoline components such as benzene, toluene, ethylbenzene and xylene (BTEX) in the environment [1–3]. Although the impacts of MTBE on human health are not well understood, it has already been listed as a possible human carcinogen [4]. In addition to the potential health risk, the compound also produces an unpleasant odor at low concentration [5,6].

The adsorption process is one of the promising techniques for the control of synthetic organic compounds (SOCs) in many environmental applications [7]. Granular activated carbon (GAC) is the most popular adsorbent used and the process has been shown to successfully remove MTBE from contaminated water [8–10]. However, poor removal efficiency may be observed in applying carbon adsorption process, especially when other SOCs co-exist with MTBE. Consequently, the carbon adsorption process may not be cost-effective for MTBE removal. The presence of natural organic matter (NOM) may also reduce the adsorption capacity and slow the kinetics while applying activated carbon in natural water [11]. To enhance the performance of adsorption and diminish the adverse effect of NOM, different types of adsorbents, such as carbonaceous resins and mordenite zeolite, were proposed for the removal of MTBE from contaminated waters.

The carbonaceous resins of Ambersorb 563 and 572 have been found to possess a superior adsorption capacity for MTBE in different water matrixes [12–14]. It was found that the two carbonaceous resins, Ambersorb 563 and 572, were promising candidates for the removal of MTBE from aqueous phase. On the other hand, the zeolite with appropriate pore size was also suggested as one of the leading adsorbents for the removal of MTBE from the aqueous phase, such as hydrophobic mordenite,

* Corresponding author. Tel.: +886 6 2364455; fax: +886 6 2752790.
E-mail address: hsuwen_hung@yahoo.com.tw (H.-W. Hung).

0304-3894/$ – see front matter © 2005 Elsevier B.V. All rights reserved.
doi:10.1016/j.jhazmat.2005.11.050

12 ring zeolite with 6.5 × 7.0 Å pore size and all-silica β zeolite with 7.1 × 7.3 Å pore size [15,16]. Based on the equilibrium experiments, mordenite and all-silica β zeolite may have better adsorption capacity of MTBE than that of activated carbon in deionized water.

Although promising equilibrium adsorption capacity of MTBE onto the carbonaceous resins and hydrophobic zeolites were verified, most studies focused on simplified water matrix such as deionized water and artificial groundwater. The adsorption behavior of MTBE in natural water is expected to be different from that in deionized water. So far, there has been much less investigation in the competition between MTBE and NOM for the adsorption on carbonaceous resins and zeolite. Additionally, the adsorption kinetics of MTBE on the adsorbents in both deionized water and natural water has been scarcely investigated. To evaluate the effectiveness of adsorption processes on the removal of MTBE-contaminated water, kinetic and equilibrium adsorption of MTBE onto two carbonaceous resins, Ambersorb 563, 572, and one zeolite, mordenite, in both deionized water and natural waters were elucidated in this study. Both kinetic and equilibrium experiments for MTBE onto the adsorbents were conducted. The data were then interpreted with appropriate equilibrium and kinetic models.

2. Materials and methods

2.1. Deionized water and natural waters

Deionized water was prepared using a Milli-Q ultra-pure-water purification system (Bedford, MA, USA). Non-purgeable dissolved organic carbon (NPDOC) for the water is smaller than 0.1 mg/L. Natural waters were collected in a groundwater source from San Tyau Liu (STL) and a surface water source from Feng Shan (FS), both located in south Taiwan. The average pH and NPDOC were 8.0 and 1.2 mg/L for STL groundwater, and were 7.7 and 2.1 mg/L for FS surface water.

2.2. Adsorbents and adsorbate

Two types of adsorbents, carbonaceous resins and mordenite zeolite, were employed in this study. The carbonaceous resins, Ambersorb 563 and Ambersorb 572, obtained from Rohm and Haas Company (Supelco, USA) were used. A mordenite type of zeolite (CBV 90A, Zeolyst International, USA) was chosen as one of adsorbents since the aperture size is comparable to the MTBE kinetic diameter. The SiO_2/Al_2O_3 ratio of the mordenite used is 90. For comparison, the commercial F400 activated carbon from Calgon Carbon, USA was also tested. The surface area, pore volume and pore size distribution was measured by nitrogen adsorption method at 77 K (ASAP 2010, Micromeritics, USA). The physical properties of the adsorbents are listed in Table 1.

MTBE-contaminated water was prepared by adding predetermined amount of reagent-grade MTBE (Janssen Chimica, Belgium) into deionized water or natural water. For analysis, a standard solution of 2000 mg/L MTBE from Supelco, USA was diluted for establishing the analytical calibration curve. Water samples were analyzed for MTBE concentration by the solid-phase micro extraction/gas chromatograph (SPME/GC) method [17]. In the SPME process, a 75 μm PDMS/Carboxen commercial fiber (Supelco, USA) was immersed into the water samples to extract MTBE. During the extraction, the temperature was controlled at 18 °C. The sample volume was 1.6 mL with addition of 25% (w/v) sodium chloride, and the extraction time was set at 60 min. The extracted fiber was injected into a GC (6890 Plus, Agilent, USA) equipped with a flame ionization detector for the determination of MTBE concentration. The detection limit of the method was determined to be 0.5 μg/L.

Table 1
Properties of the tested adsorbents

Properties	Ambersorb 563	Ambersorb 572	Mordenite
Particle density (kg/m^3)	1494[a]	1809[a]	1700[c]
Porosity (%)	52.5[b]	47.6[b]	28.0[c]
BET surface area (m^2/g)	494	958	477
Total pore volume (cm^3/g)	0.58	0.84	0.32
Micropore	0.19	0.38	0.19
Mesopore	0.15	0.22	0.10
Macropore	0.24	0.24	0.04

[a] Measured by water displace method.
[b] Estimated from about the 100 oven-dried carbonaceous resins.
[c] From D.W. Berck, Zeolites Molecular Sieves: Structure, Chemistry and Use, Wiley, New York, USA, 1974.

2.3. Adsorption experiments

The adsorption capacity of MTBE in deionized water and natural water was measured by the bottle-point technology [18]. In the equilibrium experiments, the sizes of resins were used as received (0.297–0.841 mm, or 20–50 US mesh), while that of F400 carbon were pulverized and sieved to 0.037–0.149 mm (100–400 US mesh) to ensure equilibrium status. To simplify the modeling process for the kinetic data, the resins and F400 carbon used in kinetic experiments were sieved to 0.297–0.420 mm (40–50 US mesh). Since mordenite was obtained as a powdered adsorbent, it was directly used in adsorption experiments. The mordenite adsorbent size measured by particle analyzer is 0.76 μm. Preliminary experiments showed that the adsorption capacities of carbonaceous resins and activated carbon at 4 days and 5 days were almost the same, indicating that the adsorption equilibrium may be reached within 4 days. For mordenite adsorbent, the adsorption equilibrium may be reached within 3 h. To assure equilibrium status, the experimental time of all the adsorbents used was set at 5 days. The procedures of kinetic experiment were almost the same as those of the equilibrium experiment except that more samples were taken and analyzed. The bottles were stirred magnetically at 450 rpm to reduce the liquid-phase resistance between the adsorbent and bulk solution. Blank experiments showed that MTBE concentration remained nearly constant (less than 2% of difference) during the time scale of the experimental period, revealing that the volatility of MTBE and its interaction with the bottles can be neglected. The samples of the carbonaceous resins and activated carbon, and mordenite were filtrated with 0.45 and 0.20 μm filter (Advantec MFS,

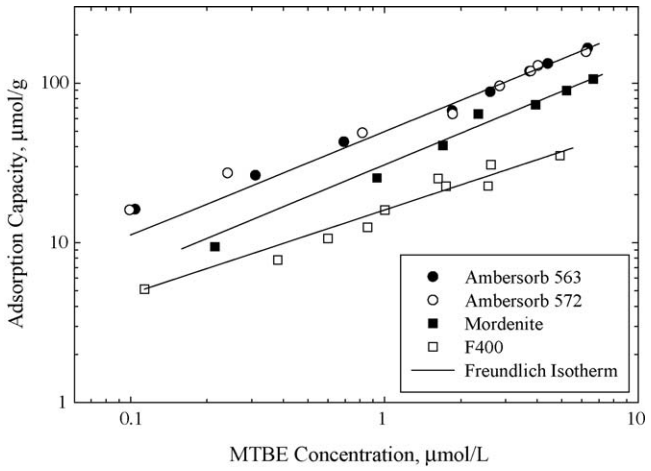

Fig. 1. MTBE isotherms of all the adsorbents tested in deionized water.

Japan), respectively, before analysis. All the experiments were conducted in a temperature-controlled chamber at 20 °C.

3. Results and discussion

3.1. Adsorption isotherms in deionized water

The MTBE isotherms for the carbonaceous resins (Ambersorb 563 and 572), and mordenite in deionized water are shown in Fig. 1. For comparison, adsorption isotherm for F400 carbon is also shown in the figure. The isotherms were linear in a log–log coordinate, implying that the Freundlich isotherm ($q = KC^{1/n}$) is adequate for describing the adsorption of MTBE onto the adsorbents in deionized water. The single-solute Freundlich parameters are listed in Table 2. To visualize the performances of different adsorbents, the adsorption capacity of MTBE at 1 μmol/L determined from the Freundlich isotherms was compared. Among the adsorbents tested, Ambersorb 563 and 572 have the highest adsorption capacity, while F400 carbon has the lowest adsorption capacity. The adsorption capacity of mordenite (30.8 μmol/g) at 1 μmol/L is almost twice the capacity of MTBE to that of F400 carbon (16.0 μmol/g), while that of Ambersorb 563 and 572 (49.7 and 52.2 μmol/g) are nearly three times that of F400 carbon. The isotherms of Ambersorb 563 and 572 are similar in the concentration range tested (0.068–6.8 μmol/L or 6–600 μg/L). The parameters of Ambersorb 563 and 572 extracted (in Table 2) are slightly different from the study of Davis and Powers [12]. This could be caused by several factors, including the artificial groundwater water matrix, and significantly higher and broader range of concentration, 600 μg/L to 1000 mg/L, used by Davis and Powers [12].

Table 2
Single-solute Freundlich isotherm parameters of the tested adsorbents

Adsorbent	K_1 (μmol/g) (μmol/L)$^{-1/n}$	$1/n_1$
Ambersorb 563	49.7	0.65
Ambersorb 572	52.2	0.61
Mordenite	30.8	0.65
F400	16.0	0.52
Ambersorb 563[a]	78.6	0.35
Ambersorb 572[a]	51.2	0.46

[a] From [12], the parameters have translated into mole base; water matrix was artificial groundwater that deionized water was buffered to a pH of about 7.2 through the addition of sodium bicarbonate.

3.2. Adsorption isotherms of resins in natural waters

The MTBE isotherms of Ambersorb 563 in STL groundwater and FS surface water are presented in Fig. 2. As shown in Fig. 2(a), the adsorption capacity of Ambersorb 563 in STL groundwater at 5.73, 2.86 and 0.54 μmol/L of initial concentration is nearly identical. Although a small deviation may be found at a low initial MTBE concentration, most experimental data follow closely the isotherm in deionized water (solid line). This small discrepancy may be caused by several factors, such as the concentration effect and extremely slow adsorption kinetics [19]. Fig. 2(a) revealed that no significant competitive adsorption between MTBE and NOM of Ambersorb 563 in STL groundwater. This observation is similar to the results from Hand et al. [20]. They pre-exposed Ambersorb 563 to NOM-laden groundwater for 10 weeks before adsorption of TCE. In their conclusions, the resin is fairly resistant to NOM fouling and the reduction of TCE adsorption capacity is insignificant [20].

Unlike that in the Ambersorb 563/STL water system, significant capacity reduction of MTBE were exhibited in Ambersorb

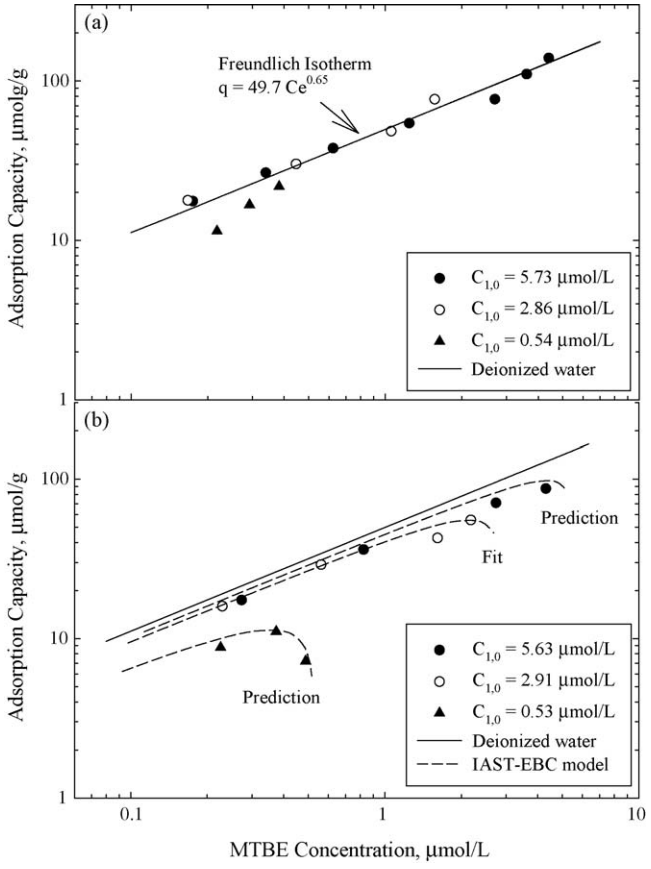

Fig. 2. MTBE isotherms of Ambersorb 563, where (a) is in STL groundwater, and (b) is in FS surface water.

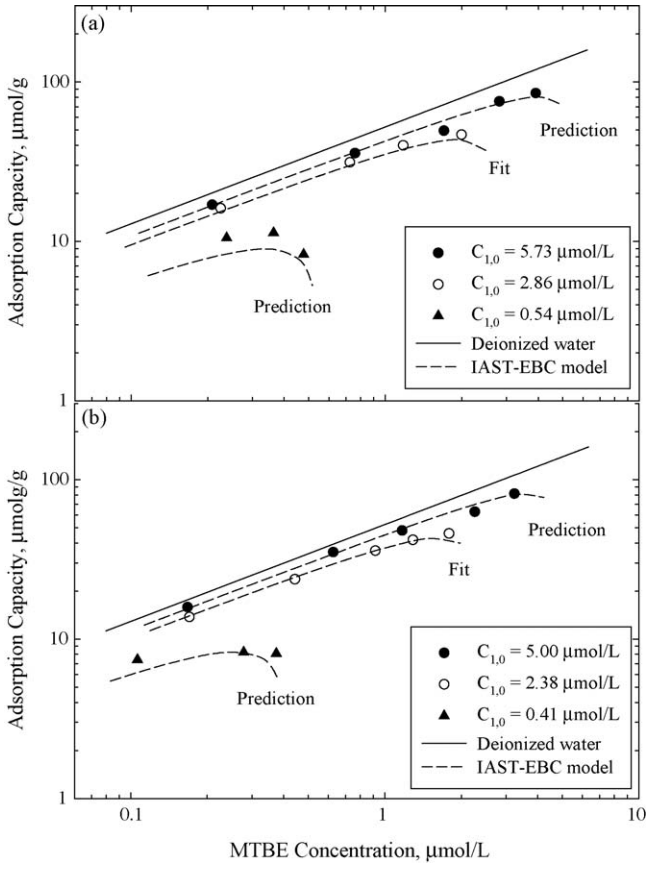

Fig. 3. MTBE isotherms of Ambersorb 572, where (a) is in STL groundwater, and (b) is in FS surface water.

563/FS, Ambersorb 572/STL and FS natural water, as presented in Figs. 2(b) and 3, respectively. The competitive adsorption between MTBE and NOM for the adsorption sites was more apparent at lower initial MTBE concentrations. The lower the initial MTBE concentration was employed, the more reduction of adsorption capacity was observed. This kind of capacity reduction is commonly present in the adsorption of organic compounds onto activated carbon in natural water systems [21,22].

The different extent of NOM competition for the two carbonaceous resins in STL and FS natural water may be caused by the NOM characteristics and pore size distribution of the adsorbent in the system [23–27]. Based on the experimental observations, it was speculated that NOM in STL groundwater may possess a more high-molecular weight fraction of NOM, while a more low-molecular weight fraction of NOM was expected in FS surface water. The low-molecular weight fraction of NOM would be able to enter the micropore and compete with MTBE for the adsorption sites [24,25]. Therefore, NOM in FS surface water has a more competitive fraction with MTBE than that in STL groundwater. This would cause the substantial reduction of MTBE capacity in FS surface water on Ambersorb 563 and 572 as shown in Figs. 2(b) and 3(b). It must be noted that discrete molecular size distribution of NOM of the two natural waters using batch ultra-filtration cells [28] were also conducted in this study (data not shown). The molecular weight cutoffs of the membranes used were 1000, 3000, 10,000, and 30,000 atomic

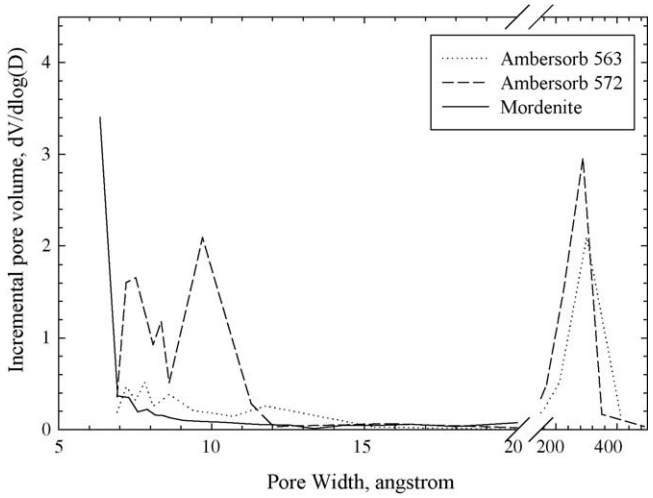

Fig. 4. Pore size distribution of the carbonaceous resins and mordenite zeolite.

mass units (AMU). However, the molecular size distribution of STL and FS natural waters was almost the same, suggesting that the decisive NOM fraction for the competition is smaller than 1000 AMU. This observation is in accordance with the results of activated carbon/organic compounds systems in the literature [24,25].

Besides NOM characteristics, the pore size distribution of adsorbents may also play an important role on the competitive adsorption [23,26,27]. The pore size distribution of the resins and mordenite calculated from MP method [29] was shown in Fig. 4. The Ambersorb 572 consisted larger micropore volume, which was concentrated in the range of 7–8 Å and 9–11 Å. The micropore volume of Ambersorb 563 was half that of Ambersorb 572 and was mainly in the range of 7–10 Å. Since the average pore size of Ambersorb 572 is larger than that of Ambersorb 563, it is expected that NOM molecules may be easier to enter the pores and thus compete with MTBE for the adsorption sites. This may explain the observation in Figs. 2(a) and 3(a), in which NOM in STL groundwater does not compete with MTBE for the adsorption sites of Ambersorb 563, but may compete in the Ambersorb 572 system.

3.3. Modeling the adsorption isotherms of resins in natural waters

Due to the competition effect between MTBE and NOM, the initial concentration of MTBE has a strong impact on its adsorption capacity in the resin/natural water systems. The isotherms conducted in a laboratory may hardly be applied to natural water systems, since the initial concentration of target organic compound in natural water may vary according to time, season and problematic episode. Therefore, to predict the equilibrium adsorption capacity of MTBE in natural water, the model should account for the effect of the initial concentration. The ideal adsorbed solution theory (IAST) combined with equivalent background compound (EBC) model, IAST-EBC, is developed to simulate the effect of initial concentration [21] in activated carbon system. The IAST-EBC model was also employed to

describe the adsorption of Ambersorb 563 and 572 in natural water. The model lumped NOM into a single component, called equivalent background compound (EBC) [21,22] and only two solutes, EBC and one target compound, were considered in the model. The IAST-EBC model combined with the Freundlich isotherm equation to describe the adsorption of both EBC and the target compound onto the adsorbent in deionized water can be expressed as [21]:

$$C_{1,0} - q_1 C_c - \frac{q_1}{q_1 + q_2}\left(\frac{n_1 q_1 + n_2 q_2}{n_1 K_1}\right)^{n_1} = 0 \quad (1)$$

$$C_{2,0} - q_2 C_c - \frac{q_2}{q_1 + q_2}\left(\frac{n_1 q_1 + n_2 q_2}{n_2 K_2}\right)^{n_2} = 0 \quad (2)$$

in which subscripts 1 and 2 represent a target compound, MTBE and EBC, respectively; $C_{i,0}$ is the initial concentration of *i* compound; C_c is adsorbent dosage; q_i is solid-phase concentration; and K_i and n_i are the constants of single-solute Freundlich isotherm ($q = KC^{1/n}$). Following the similar procedure Najm et al. proposed [21], the EBC parameters were extracted from the isotherms of Ambersorb 563 at 2.86 and 2.91 μmol/L in STL groundwater and FS surface water, respectively, while the concentrations at 2.86 and 2.38 μmol/L were used for Ambersorb 572 in the two natural waters. It must be noted that the isotherm for extracting the parameters was arbitrarily selected and no significant difference of model predictions were found using different sets of parameters. The extracted model parameters are listed in Table 3. As shown in Figs. 2 and 3, the IAST-EBC model predicted the experimental data very well for both Ambersorb 563 and 572 at different initial MTBE concentrations in both STL groundwater and FS surface water. Moreover, the model delineated the isotherm curvature at high MTBE concentration with low adsorbent dosage. It should be noted that the model parameters for Ambersorb 563/STL groundwater was also extracted and are given in Table 3. Although no significant competitive adsorption was found for the Ambersorb 563/STL groundwater system, the model predictions were almost identical to the isotherm in deionized water regardless of the MTBE initial concentrations employed (predictions not shown). So far, the IAST-EBC model was only focused on the adsorbent of activated carbons in different water matrix. Based on the results, application of the IAST-EBC model may be extended to the carbonaceous resins, Ambersorb 563 and 572, and may adequately predict the isotherm curvature at high target compound concentrations with low adsorbent dosage.

Table 3
The IAST-EBC parameters for all the carbonaceous resins in natural waters

Adsorbent	Water matrix	$C_{2,0}$ (μmol/L)	K_2 (μmol/g)(μmol/L)$^{-1/n}$	$1/n_2$
Ambersorb 563	STL groundwater	4.86×10^{-7}	29370	0.65
	FS surface water	7.4	2511	0.65
Ambersorb 572	STL groundwater	3.2	5675	0.61
	FS surface water	1.9	5754	0.61

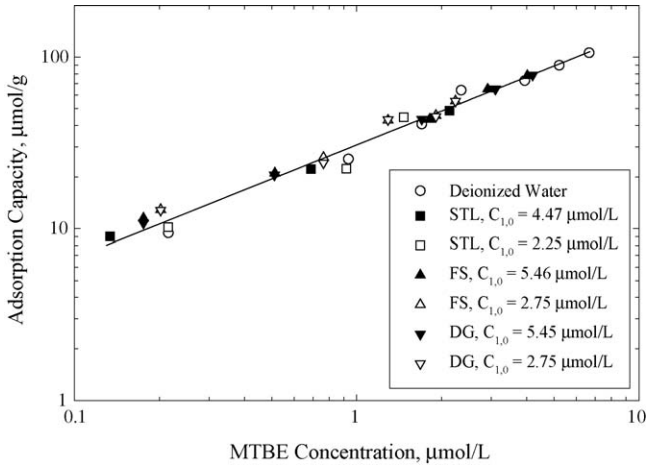

Fig. 5. MTBE isotherms of mordenite in deionized water and natural waters.

3.4. Adsorption isotherms of mordenite in natural waters

The MTBE isotherms of mordenite with $SiO_2/Al_2O_3 = 90$ in FS surface water is exhibited in Fig. 5. For comparison, the figure also includes the experimental data of MTBE in deionized water, STL groundwater and DG River water from the study of Hung et al. [30]. The results revealed that the experimental data in natural waters for different initial concentrations were nearly identical with the solid line, the single-solute Freundlich isotherm, indicating that NOM did not compete with MTBE for the adsorption sites. This may be attributed to the molecular sieve effect which occurred within the adsorbent. Unlike porous adsorbents, such as activated carbon and the two resins used in this study, the aperture of mordenite zeolite is highly uniform and concentrated, as shown in Fig. 4. Assuming that the average molecular weight is 1200 AMU for STL groundwater and FS surface water (calculated from molecular size distribution data), NOM density is 1 g/cm^3, and NOM molecules are spherical [26], the average molecular diameter is estimated to be 16 Å. This size is much larger than the internal channel of mordenite, 6.5 × 7.0 Å. Therefore, most NOM molecules are expected not able to enter the apertures. In fact, for NOM to enter the apertures of 7.0Å, the molecular weight is calculated to be around 100 AMU. This small molecular weight fraction of NOM is normally very small, as reported in the literature [25–27]. Since MTBE molecule has a kinetic diameter (6.2 Å) close to but slightly smaller than the internal channel of the mordenite (6.5 × 7.0 Å), this will make MTBE molecules excellently fit into the 12-membered oxygen ring pores of the mordenite.

3.5. Adsorption kinetics

To understand the transport and adsorption of MTBE onto the carbonaceous resins and mordenite in both deionized and natural water, adsorption kinetic experiments were conducted and modeled. The pore diffusion model (PDM) coupled with Freundlich isotherm was employed to simulate the adsorption kinetics of the resins used in different water matrix. The PDM has been widely employed to simulate the adsorption kinetics for

porous adsorbents in the aqueous phase [31]. Detailed assumptions of PDM in a batch adsorption system used in this study can be found elsewhere [31]. The transient equation describing the transport of adsorbate molecules within adsorbents for a batch adsorption system can be expressed as:

$$\varepsilon_p \frac{\partial C}{\partial t} + (1-\varepsilon_p)\rho_p \frac{\partial q}{\partial t} = \frac{1}{r^2}\frac{\partial}{\partial r}\left(r^2 D_p \frac{\partial C}{\partial r}\right) \quad (3)$$

where ε_p is the grain porosity, ρ_p is the particle density of the adsorbent, r is the radial coordinate of the adsorbent, D_p is the effective pore diffusivity of the adsorbate, C is the aqueous concentration of adsorbate within the pore, q is the solid-phase concentration of adsorbate and t is time. To speculate the complexity of pore structure, the tortuosity factor was used to determine the extent of the tortuous path and pore constrictions within the adsorbent. The tortuosity factor (τ) can be given as:

$$\tau = \frac{\varepsilon_p D_m}{D_P} \quad (4)$$

where D_m is molecular diffusivity. In this study, the molecular diffusivity of MTBE estimated from the Wilke–Chang equation [32] was 8.0×10^{-6} cm^2/s; relevant physical parameters of the adsorbents for the model input are listed in Table 1.

For mordenite zeolite, the PDM may not be appropriate for describing the transport of MTBE in the small and uniform cylindrical aperture of the adsorbent particles. Instead, a micropore diffusion equation as described in Ruthven [33] is used to qualitatively simulate the adsorption kinetics of MTBE in deionized water, STL groundwater and FS surface water. The transient diffusion equation of adsorbate molecules within spherical microporous adsorbents can be expressed as [33]:

$$\frac{\partial q}{\partial t} = \frac{1}{r^2}\frac{\partial}{\partial r}\left(r^2 D_c \frac{\partial q}{\partial r}\right) \quad (5)$$

where D_c is the intracrystalline diffusivity of the adsorbate, q is the solid-phase concentration and t is the time. To solve the two diffusion models, the algorithm employed is modified from a numerical code BATCH developed by Tien [34].

The Freundlich isotherm determined from the IAST-EBC model for specific initial concentration in natural water was used to describe local equilibrium in the model. To fit the model to the experimental data, only effective pore diffusivity and intracrystalline diffusivity was adjusted. The extracted diffusivity was further used to predict the adsorption kinetics for different initial concentrations. The best-fitted effective diffusivity (D_p) and tortuosity factor (τ) of the carbonaceous resins are listed in Table 4. Both best-fitted and predicted models were plotted against the experimental kinetic data for Ambersorb 563 in deionized water, STL groundwater and FS surface water, and are shown in Fig. 6. Similar simulations were also performed for Ambersorb 572 (figure not shown). Not only the fitted models followed the experimental data fairly well, as shown in the figure, but also the predicted models reasonably described the adsorption kinetics for different initial concentrations of MTBE. This would suggest that the effective pore diffusivity is independent of MTBE initial concentration and the adsorbent dosage. Although the effective pore diffusivity for the cases of Ambersorb 563 and

Table 4
The kinetic parameters of MTBE within carbonaceous resins in different water matrix

Adsorbent	Water matrix	D_p (cm^2/s)	τ
Ambersorb 563	Deionized water	3.4×10^{-6}	1.2
	STL groundwater	2.1×10^{-6}	2.0
	FS surface water	2.1×10^{-6}	2.0
Ambersorb 572	Deionized water	3.1×10^{-6}	1.2
	STL groundwater	1.7×10^{-6}	2.3
	FS surface water	2.9×10^{-6}	1.3

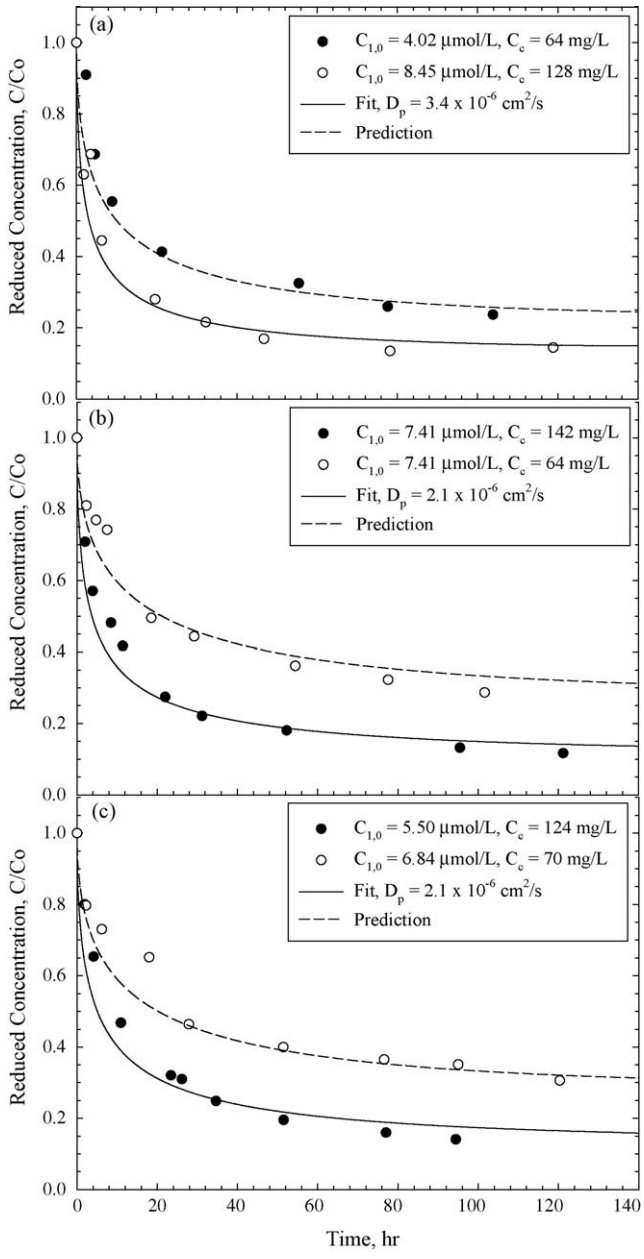

Fig. 6. Adsorption kinetics of MTBE onto Ambersorb 563, where (a) is in deionized water, (b) is in STL groundwater and (c) in FS surface water.

572 was higher in deionized water, no significant difference of D_p was observed in the cases of deionized water and natural waters. This may be interpreted as carbonaceous resins possess numerous mesopore and macropore volumes which facilitate the access of MTBE to the inner micropore, as shown in Table 1. The tortuosity factor of Ambersorb 563 and 572 was between 1.2 and 2.3, somewhat smaller than general magnitude (2–6) for porous adsorbents [33], suggesting that intraparticle diffusion takes place along the radial direction as Eq. (3) implied [33,34].

The adsorption kinetic of MTBE within mordenite in FS surface water is depicted and simulated by micropore diffusion model, as shown in Fig. 7. For comparison, Fig. 7 also includes the experimental data of MTBE in deionized water and STL groundwater from the study of Hung et al. [30]. The Freundlich isotherm in deionized water was directly used in the model. The models were able to capture the adsorption kinetics of MTBE onto mordenite for all the water matrix tested. The best-fitted intracrystalline diffusivity of MTBE in deionized water is 2.0×10^{-13} cm^2/s, while that in STL groundwater and FS surface water is 2.0×10^{-14} and 6.0×10^{-14} cm^2/s, respectively. The adsorption kinetics in this case was much slower than that for the carbonaceous resins. In the case of deionized water, equilibrium time for mordenite (0.5 h) is about two order of magnitudes smaller than that for the carbonaceous resins (100 h). For the adsorption in natural waters, the diffusivity of MTBE was much slower than that in deionized water, only 1/10 in STL groundwater and 1/3 in FS surface water. This may be attributed to the fact that NOM molecules may be too large to enter the apertures, as shown in previous section. However, they may instead block the entrance of the apertures. Although some of the diffusional pathways were hindered due to the surface blockage, the intraparticle apertures were still connected to each other. Therefore, the adsorption kinetics was slow in natural water systems. However, the adsorption capacity would be the same for the cases in deionized water and natural waters, as shown in Fig. 5.

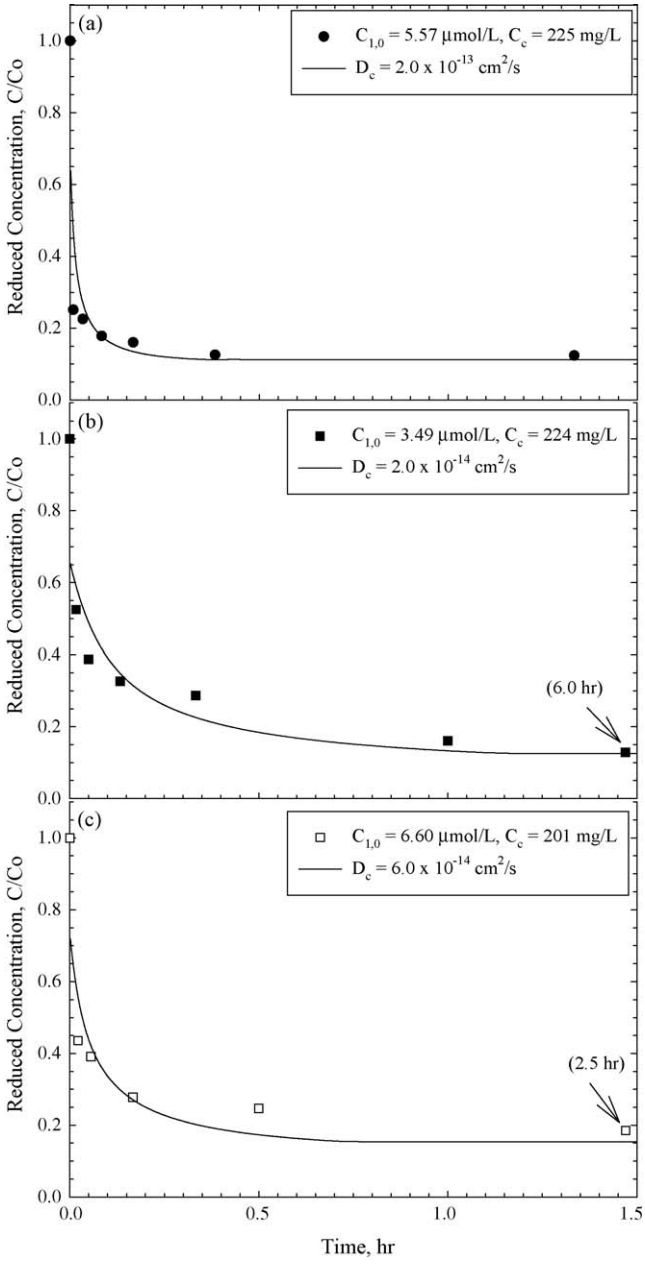

Fig. 7. Adsorption kinetics of MTBE onto mordenite, where (a) is in deionized water, (b) is in STL groundwater and (c) is in FS surface water.

4. Conclusions

According to the experimental and modeling observation, NOM may compete with MTBE for the adsorption sites within the adsorbents tested. The competition effect is substantial for Ambersorb 563 in FS water, and Ambersorb 572 in both STL and FS waters. However, no significant competition was present for the systems of Ambersorb 563 in STL water, and mordenite in the three natural waters. This may be attributed to the fact that NOM molecules were too large to enter the pores of the two adsorbents, and thus, the adsorption capacity of MTBE was not affected. The pore sizes of the adsorbents also affect the transport of MTBE into the adsorbents. A much faster adsorption kinetics of MTBE onto the two resins tested was observed compared to that onto the mordenite zeolite. The presence of NOM near aperture entrances of mordenite may reduce the number of transport paths for MTBE and slow the adsorption kinetics for MTBE in natural waters. Although the adsorption equilibrium was influenced by the presence of NOM, for the adsorbents tested, the IAST-EBC model successfully predicted the adsorption capacity of MTBE in natural waters under different initial concentrations. When combined the IAST-EBC model with the pore diffusion and micropore diffusion model for describing the transport of MTBE into the carbonaceous resins and mordenite zeolite, respectively, the models excellently predicted the adsorption kinetics of the resins and zeolite employed in different water matrix. This may further substantiate the applicability of the models.

Acknowledgment

This work was supported by National Science Council, Taiwan, under grant number NSC91-2211-E-006-026.

References

[1] P.J. Squillace, J.S. Zogorski, W.G. Wilber, C.V. Price, Preliminary assessment of the occurrence and possible sources of MTBE in groundwater in the United States 1993–94, Environ. Sci. Technol. 30 (1996) 1721–1730.

[2] R.W. Gullick, M.W. LeChevallier, Occurrence of MTBE in drinking water sources, J. Am. Water Works Assoc. 92 (2000) 100–113.

[3] T. Shih, Y. Rong, T. Harmon, M. Suffet, Evaluation of the impact of fuel hydrocarbons and oxygenates on groundwater resources, Environ. Sci. Technol. 38 (2004) 42–48.

[4] OEHHA (Office of Environmental Health Hazard Assessment), Public Health Goal for Methyl Tertiary Butyl Ether (MTBE) in Drinking Water, Pesticide and Environmental Toxicology Section, California EPA, USA, 1999.

[5] W.F. Young, H. Horth, R. Crane, T. Ogden, M. Arnott, Taste and odour threshold concentrations of potential potable water contaminants, Water Res. 30 (1996) 331–340.

[6] A.J. Stocking, I.H. Suffet, M.J. Mcguire, M.C. Kavanaugh, Implications of an MTBE odor study for setting drinking water standards, J. Am. Water Works Assoc. 93 (2001) 95–105.

[7] W.J. Weber, P.M. Mcginley, L.E. Katz, Sorption phenomena in subsurface systems: concepts, model and effects on contaminant fate and transport, Water Res. 25 (1991) 499–528.

[8] M.J. Wilhelm, V.D. Adams, J.G. Curtis, E.J. Middlebrooks, Carbon adsorption and air-stripping removal of MTBE from river water, J. Environ. Eng. 128 (2002) 813–823.

[9] T.C. Shih, M. Wangpaichitr, M. Suffet, Evaluation of granular activated carbon technology for the removal of methyl tertiary butyl ether (MTBE) from drinking water, Water Res. 37 (2003) 375–385.

[10] J. Sutherland, C. Adams, J. Kekobad, Treatment of MTBE by air stripping, carbon adsorption, and advanced oxidation: technical and economic comparison for five groundwaters, Water Res. 38 (2004) 193–205.

[11] H. Sontheimer, J.C. Crittenden, R.S. Summers, Activated carbon for water treatment, in: DVGW-Forschungsstelle, second ed., Engler-Bunte-Institut, University of Karlsruhe, Karlsruhe, Germany, 1988.

[12] S.W. Davis, S.E. Powers, Alternative sorbents for removing MTBE from gasoline-contaminated ground water, J. Environ. Eng. 126 (2000) 354–360.

[13] S.H. Lin, C.S. Wang, C.H. Chang, Removal of methyl *tert*-butyl ether from contaminated water by macroreticular resin, Ind. Eng. Chem. Res. 41 (2002) 4116–4121.

[14] T. Shih, M. Wangpaichitr, M. Suffet, Performance and cost evaluations of synthetic resin technology for the removal of methyl tert-butyl ether from drinking water, J. Environ. Eng. 131 (2005) 450–460.

[15] M.A. Anderson, Removal of MTBE and other organic contaminants from water by sorption to high silica zeolites, Environ. Sci. Technol. 34 (2000) 725–727.

[16] S. Li, V.A. Tuan, R.D. Noble, J.L. Falconer, MTBE adsorption on all-silica β zeolite, Environ. Sci. Technol. 37 (2003) 4007–4010.

[17] C. Achten, W. Puttmann, Determination of methyl *tert*-butyl ether in surface water by use of solid-phase microextration, Environ. Sci. Technol. 34 (2000) 1359–1364.

[18] S.J. Randtke, V.L. Snoeyink, Evaluating GAC adsorption capacity, J. Am. Water Works Assoc. 75 (1983) 406–413.

[19] G.S. Wang, Removal of atrazine from drinking water by activated carbon adsorption, Doctoral Thesis, State University of New York Albany, 1994.

[20] D.W. Hand, J.A. Herlevich, D.L. Perram, J.C. Crittenden, Synthetic adsorbent versus GAC for TCE removal, J. Am. Water Works Assoc. 86 (1994) 64–72.

[21] I.N. Najm, V.L. Snoeyink, Y. Richard, Effect of initial concentration of a SOC in natural water on its adsorption by activated carbon, J. Am. Water Works Assoc. 83 (1991) 57–63.

[22] D.R.U. Knappe, Y. Matsui, V.L. Snoeyink, P. Roche, M.J. Prados, M.M. Bourbigot, Predicting the capacity of powdered activated carbon for trace organic compounds in natural waters, Environ. Sci. Technol. 32 (1998) 1694–1698.

[23] G. Newcombe, J. Morrison, C. Hepplewhite, Simultaneous adsorption of MIB and NOM onto activated carbon. I. Characterisation of the system and NOM adsorption, Carbon 40 (2002) 2135–2146.

[24] G. Newcombe, J. Morrison, C. Hepplewhite, D.R.U. Knappe, Simultaneous adsorption of MIB and NOM onto activated carbon. II. Competitive effects, Carbon 40 (2002) 2147–2156.

[25] Q.L. Li, V.L. Snoeyink, B.J. Marinas, C. Campos, Elucidating competitive adsorption mechanisms of atrazine and NOM using model compounds, Water Res. 37 (2003) 773–784.

[26] C. Pelekani, V.L. Snoeyink, Competitive adsorption in natural water: role of activated carbon pore size, Water Res. 33 (1999) 1209–1219.

[27] Q.L. Li, V.L. Snoeyink, B.J. Marinas, C. Campos, Pore blockage effect of NOM on atrazine adsorption kinetics of PAC: the roles of PAC pore size distribution and NOM molecular weight, Water Res. 37 (2003) 4863–4872.

[28] B.E. Logan, Q. Jiang, Molecular size distributions of dissolved organic matter, J. Environ. Eng. 116 (1990) 1046–1062.

[29] S. Lowell, J.E. Shields, Powder Surface Area and Porosity, second ed., John Wiley & Sons, New York, USA, 1984.

[30] H.W. Hung, T.F. Lin, C. Baus, F. Sacher, H.J. Brauch, Competitive and hindering effects of natural organic matter on the adsorption of MTBE onto activated carbons and zeolites, Environ. Technol. 26 (2005) 1371–1382.

[31] T.F. Lin, J.K. Wu, Adsorption of arsenite and arsenate within activated alumina grains: equilibrium and kinetics, Water Res. 35 (2001) 2049–2057.

[32] W.J. Weber, F.A. DiGiano, Process Dynamics in Environmental Systems, John Wiley & Sons, New York, USA, 1996.

[33] D.M. Ruthven, Principles of Adsorption and Adsorption Processes, John Wiley & Sons, New York, USA, 1984.

[34] C. Tien, Adsorption Calculations and Modeling, Butterworth-Heinemann, Boston, USA, 1994.